Open Access

Research Article

PRNANO

Precis. Nanomed. 7(1):1252-1263, 2024

ANDOVER HOUSE

Magnetic resonance imaging of mesenchymal stem cell – migration towards glioblastoma using nano-calcium phosphate contrast agent

Ida M. Anna, Genekehal Siddaramana Gowd, Anusha Ashokan, Maneesh Manohar, Shantikumar V Nair, Kishore Bhakoo, Manzoor Koyakutty*

Amrita School Of Nanosciences and Molecular Medicine, Amrita Vishwa Vidyapeetham, Kochi, Kerala – 682041, India

Submitted: November 1, 2023 Accepted: February 19, 2024 Published: February 20, 2024

Graphical Abstract

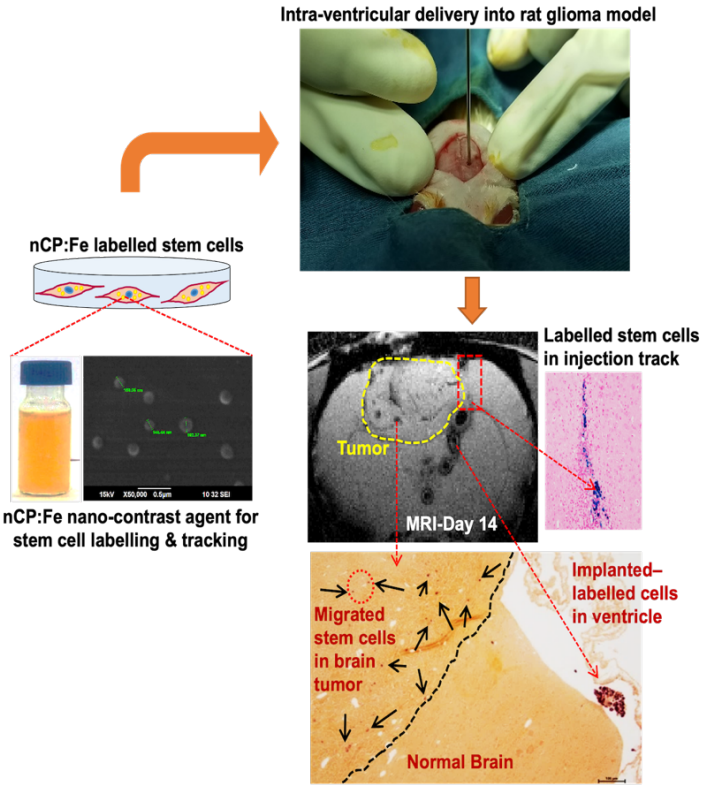

Abstract

Tracking stem cell homing to the brain, their infiltration, and brain tissue distribution are critical for evaluating the efficacy of stem cell-based anti-glioma therapy. Here, we report the use of a biomineral magnetic nano-contrast agent, Fe-doped calcium phosphate nanoparticles (nCP:Fe), to label mesenchymal stem cells (MSCs) and track their migration toward brain tumors using magnetic resonance imaging (MRI). nCP:Fe labeled MSCs implanted intra-ventricularly in a rat C6-glioma model showed longitudinal migration towards tumor region over 14 days, detected as hypointense signals in T2/T2* weighted-MR images, which was confirmed *ex vivo* using histological staining. Although a small fraction of implanted MSCs migrated to the tumor site, the study demonstrates that MRI tracking of stem cells using nCP:Fe nano-contrast agent will facilitate a better assessment of the efficacy of stem cell-guided anti-tumor therapy.

Keywords:

Glioma, stem cells, tumor migration, calcium phosphate nanoparticles, magnetic resonance imaging

* Corresponding Author: Manzoor Koyakutty, E-mail: manzoork@acnsmm.aims.amrita.edu

Rationale, Purpose, and Limitations

This study aims to analyze the possibility of non-invasive tracking of the migration of magnetically labeled stem cells toward brain tumors. The study demonstrates that a bio-mineral MR contrast agent, nano-calcium phosphate doped with iron (nCP:Fe), can be used to label mesenchymal stem cells (MSCs) and delineate their pattern of infiltration into the tumor by MRI after intra-ventricular injection in an orthotopic rat-glioma model. However, a detailed investigation of the *in vivo* fate of the injected cells, as well as their survival, functionality, immune response, and long-term effect, has to be examined. Overall, this study indicates the potential of nCP:Fe nano-contrast agent for labeling stem cells and tracking their migration towards solid brain tumors using MRI, which may benefit optimizing and improving MSC-based anti-glioma therapies.

Introduction

Stem cell therapy has been reported as a promising strategy for the management of malignant brain tumors, especially *glioblastoma multiforme* (GBM).[1]–[3] Several studies reported that, among stem cells, mesenchymal stem cells (MSCs) possess unique tumor-targeting properties (tropism), and they can migrate towards glioma after intracranial or intra-arterial/intravenous implantation with a maximum reported migration efficiency of ~ *20%*.[4]–[6] Furthermore, studies have demonstrated that migrated MSCs can infiltrate and exert an inhibitory effect on tumor progression by impairing angiogenesis or inducing apoptosis in tumor mass.[7]–[9] However, some reports pointed out that MSCs may also show bi-directional and paradoxical immune-suppressive effects leading to enhanced tumor growth depending on the tumor microenvironment and their interaction with tumor cells.[10],[11] Therefore, monitoring the efficiency of stem cell migration, intratumoral distribution, and their effect on tumor growth are essential considerations in optimizing stem-cell-based anti-tumor therapies. In this context, real-time, non-invasive tracking of implanted stem cells in the brain has significant utility.

Magnetic resonance imaging (MRI) has become a widely preferred imaging modality for tracking transplanted cells *in vivo* because of its high spatio-temporal resolution and absence of ionizing radiation.[12] Moreover, MRI is used routinely in clinical diagnosis and post-treatment surveillance of malignant brain tumors. Therefore, MR imaging can be a reliable, non-invasive technique to image and track the tumor-tropism of intra-cerebrally-implanted stem cells serially, provided the cells are pre-labeled with biocompatible magnetic contrast agents. In the past decade, iron oxide nano-contrast agents, principally superparamagnetic iron oxide nanoparticles (SPIONs), have been used as T2-contrast agents to label and track stem cells using MRI.[13]–[15] Recently, some studies have used this strategy successfully to demonstrate the migration of stem cells to malignant glioma in experimental tumor models.[6],[16],[17] However, reports are stating that excess doses of iron in SPION-labeled cells can cause reactive oxygen species (ROS)-mediated oxidative damage, leading to an adverse impact on significant stem cell functions.[18],[19] Moreover, many of the SPION-based commercial MR contrast agents such as Feridex® IV, Resovist®, Combidex®, and Sinerem® have been withdrawn due to their toxicity profiles.[20], [21]

Previously, our group reported a biomineral-based nano-contrast agent, namely doped calcium phosphate nanoparticles, and explored its use for theranostic and imaging applications.[22]–[25] Recently, we have also reported the potential of this nano-contrast agent, calcium phosphate nanoparticles doped with 9.8 wt% of Fe^{3+} (nCP:Fe), to label stem cells and demonstrated its feasibility to track cell migration, post-intra-cerebral implantation in a lipopolysaccharide (LPS) induced inflammatory rat brain model, using MRI.[26] We found that the labeled MSCs migrated from their implanted site toward the site of inflammation, which was detected as a progressively increasing dark signal at the inflammatory region for up to 30 days. The present study demonstrates the MRI-based tracking of nCP:Fe-labeled stem cells during their migration towards an aggressively growing orthotopic brain tumor after intra-ventricular implantation.

Results and Discussion

We have synthesized nCP:Fe nanoparticles using a wet-chemical method, as discussed in our previous study.[26] The nanoparticles (NPs) are redispersed in milli. Q water showed an average hydrodynamic size of 134.3 ± 62.2 nm (Figure 1A) and a negative surface charge of -16.7 ± 6.50mV (Figure 1B). The scanning electron microscope (SEM) image (Figure 1C) indicated the formation of spherical NPs with an average size range of 140-195nm. The magnetic properties of nCP:Fe were studied in detail in our previous report on demonstrating the feasibility of these NPs for MRI-assisted radiofrequency ablation of liver tumors.[23] The vibrating sample magnetometer analysis indicated that nCP:Fe exhibited a paramagnetic behaviour with a dose-dependent increase in its paramagnetic property according to the increased doping concentration of Fe^{3+} ions.[23] Further, to investigate the application potential of nCP:Fe NPs in the context of cell labeling and tracking, we examined the T2-contrast properties using 7.0 T preclinical MRI in our previous study.[26] As reported, the T2 and T2* weighted images showed reduced proton relaxation time (increase in dark signal) with increased nCP:Fe NPs concentrations.[26] These NPs were used to label MSCs isolated from rat bone marrow by co-incubating the cells with NPs in opti-MEM media. Following the optimized labeling conditions reported in our earlier study, we labeled MSCs with 100 µg/mL of nCP:Fe for 6 hours, and the cellular labeling was analyzed using Prussian-blue staining.[26] In the Prussian-blue image (Figure 1D), the blue spots seen in the cells clearly indicate the presence of nCP:Fe within the labeled cells.

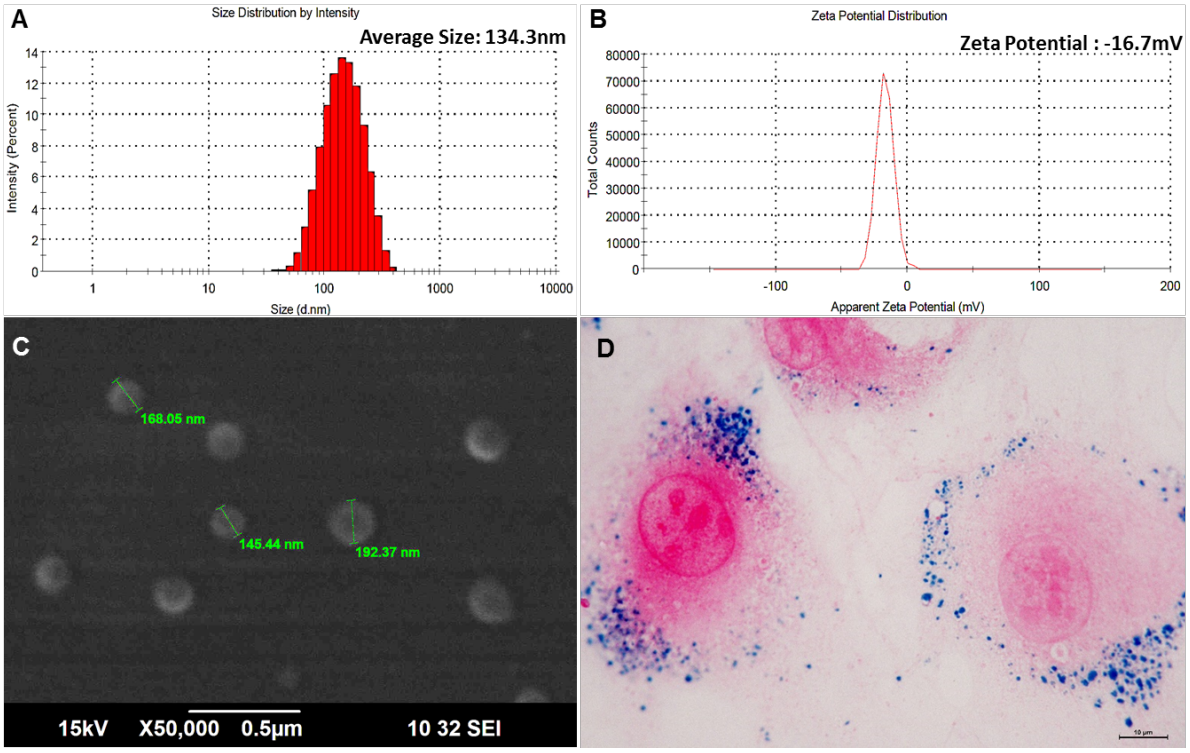

Figure 1. A) DLS, B) Zeta potential, and C) SEM image of nCP:Fe D) Prussian-blue staining of MSCs labeled with nCP:Fe, at optimized labeling conditions (100 µg/mL nCP:Fe; 06 hrs incubation time)

In the previous study, we showed that this protocol has resulted in ~ 87% labeling efficiency with ~ 22.34 pg Fe/cell (quantified using ICP), which was good enough to provide detectable T2-contrast for labeled stem cells in the brain.[26] In addition, we have demonstrated that nCP:Fe labeling has no negative impact on stem cell viability, proliferation potential, and neuronal differentiation potential in vitro.[26] Further, the low ROS levels, unaltered surface-marker expression, and intact cellular cytoskeleton arrangement in labeled cells indicated the compatibility of nCP:Fe with stem cells.[26] Though the transverse relaxivity (r_2) of nCP:Fe

(~16.132 $mM^{-1}sec^{-1}$) was low compared to SPIONs available in market (such as Feridex, $r_{2\ at\ 7T}$:166.71 $mM^{-1}sec^{-1}$ and Feraheme,$r_{2\ at\ 7T}$:68 $mM^{-1}sec^{-1}$), nCP:Fe delivered evident T2 contrast for labeled stem cells with an *in vitro* detectability up to 10^4 cells, and *in vivo* MR image-ability in brain up to 30 days, at the concentration of ~ 22.34 pg Fe/cell.[26] Thus, the low doping concentration of Fe^{3+} ions (~ 9.81 wt%) within the NPs and its biomineral composition makes nCP:Fe a promising biocompatible nano-contrast agent for stem cell labeling and tracking

To evaluate the response of labeled stem cells on the growth of glioma cells *in vitro*, a preliminary study was conducted by co-culturing nCP:Fe labeled stem cells with carboxyfluorescein succinimidyl ester (CFSE)-stained rat C6-glioma cells, and their interaction was monitored live for 18hrs using a confocal microscope. The fluorescently (CFSE-Green) stained C6-glioma cells were attached to the culture plate (denoted as 'G' in Figure 2A), and an equal number of nCP:Fe labeled MSCs (seen as round-shaped suspended cells, denoted as 'M' in Figure 2B) were seeded onto the culture dish for the study. Interestingly, the glioma cells that were attached to the plate (with spindle-shaped morphology) were found floating after 3–4 hrs of the co-culture (denoted by the yellow arrows in Figure 2C), and the labeled MSCs started attaching to the plate, followed by attaining its typical morphology (Figure 2C). Further, it was visually noticed that, by 6-8 hours, most of the glioma cells were detached from the culture plate and suspended in the media (Figure 2D), while the stem cells were completely attached to the plate.

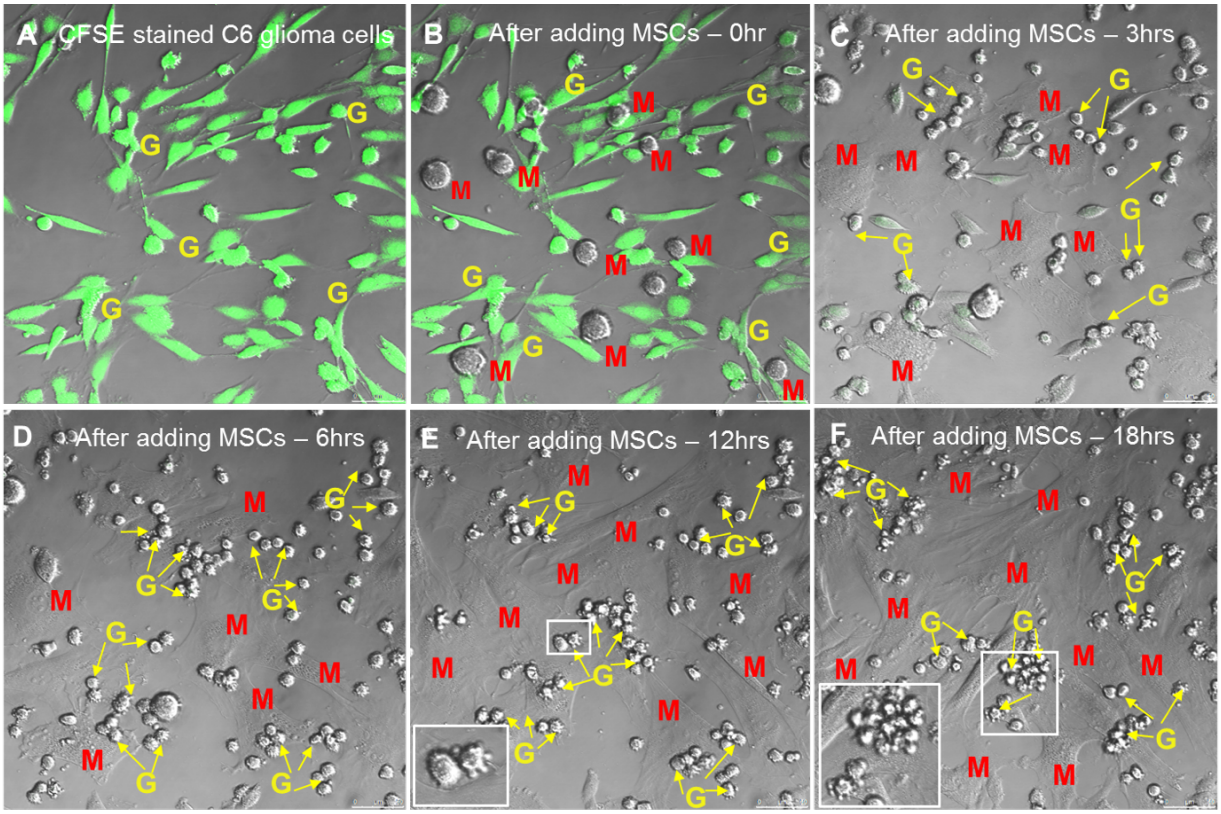

Figure 2. Microscopic images of labeled MSCs co-cultured with C6-glioma cells in vitro A) C6-glioma cells (green) stained with CFSE (denoted as 'G') B) labeled MSCs added into the culture plate (denoted as 'M'). Microscopic images of the cells after C) 3hrs, D) 6hrs, E) 12hrs, and F)18hrs of co-culture. (glioma cell detached and suspended in culture is indicated by yellow arrows, denoted as 'G') (scale bar represents 50 µm, Images acquired from the same field of view using confocal live-cell imaging under CO_2 incubation at 37°C)

Over a period, the suspended glioma cells were found to have cell shrinkage (Figure 2E with the zoomed image of the inset below) together with membrane blebbing (Figure 2F with a zoomed image of the inset below),

whereby these morphological changes indicated the occurrence of apoptotic cell death in glioma cells [27]–[29]. Meantime, the labeled -MSCs attached to the plate were divided and expanded without any observable negative impact on their viability (Figure 2F and supplementary data – Movie S1). These observations indicated that the labeled MSCs exerted an inhibitory effect on the growth of glioma cells *in vitro*.

Several studies have investigated the anti-tumor properties of MSCs, both *in vitro* and *in vivo,* and proposed their inhibitory effect on tumor cells through the induction of apoptosis.[9],[30] Yang et al. demonstrated that MSC-conditioned media could significantly inhibit the growth of human U251 glioma cells *in vitro* by inducing apoptosis in cells by up-regulating apoptotic genes (caspase-3 and caspase-9) and down-regulating anti-apoptotic genes (survivin and XIAP).[31] In another study, Ho et al. reported that MSCs inhibited the growth of human glioma cells and patient-derived primary glioma cells *in vitro* by inducing apoptosis.[7] Our finding also suggested that nCP:Fe labeled-MSCs could exert an inhibitory effect on the tumor cells *in vitro,* and the anti-tumor property of MSCs is not affected adversely by the NP labeling. However, cytochemical determination and quantitative assessment of apoptotic cell death of glioma cells have to be evaluated, and the specific cellular mechanism underlying the observed inhibitory effect by MSCs needs further investigation.

Furthermore, to track and delineate the migratory pattern of labeled MSCs toward glioma, we established an orthotopic tumor in a rat brain by injecting C6-glioma cells in the right cerebral hemisphere, as reported previously.[32] After seven days, we implanted nCP:Fe labeled- MSCs into the left lateral ventricle and monitored the mobility of stem cells using MRI for 14 days. Figure 3 represents the MRI images of different rat brain sections (axial, coronal, and sagittal sections) taken on Days 0-14, post-stem cell implantation. On the day of stem cell implantation (7^{th} day of tumor induction), a small lesion was seen at the site of injection of glioma cells (G-SOI) in T2-weighted MR images (Figure 3A). Immediately after the labeled cells were delivered into the left lateral ventricle, hypointense signals (red arrows) were detected in T2-weighted MR images, which were enhanced in T2*-weighted images of axial sections (Figure 3A-lower panel). The labeled cells, denoted as 'LC,' were dispersed in the cerebrospinal fluid (CSF) in the ventricular region, making the whole area dark. Respective coronal and sagittal-section-MR images also showed dark regions of labeled cells. The T2 values at different brain regions were measured from the T2 maps. The T2 value at the left-ventricular region, where the labeled cells were injected, was 39.2 msec, which was significantly lower than the typical T2 value of the CSF-filled right-ventricular space (103.9 msec) and the cerebral striatum (50.7 msec), where cell injection was not done. The substantial reduction in T2 value clearly indicates the presence of labeled cells in the left ventricles.

On Day 5 (the 12^{th} day after tumor cell inoculation), the orthotopic tumor was distinguished as a distinct mass (blue dotted lines, denoted as 'G') with a hyper-intense signal in the T2-MR image (Figure 3B). This was reflected in the T2 value at the tumor region (68.3 msec), which is comparatively higher than that of the striatum (50.7 msec). A few small discontinuous dark curves appeared near the tumor margin. A few dark spots were seen within the tumor region (yellow-dotted circles in Figure 3B) in the axial T2/T2*-MR images (in consecutive sections), indicative of the presence of labeled cells in the tumor region (denoted as 'M-LC-G' in Figure 3B). The T2 value at this hypointense region was 45.2 msec, which was relatively lower than that of the tumor mass (68.3 msec), which makes the area distinguishable from the fairly bright tumor background. These dark signals were also observed in their respective coronal and sagittal-section MR images, indicating that although most of the implanted labeled MSCs remained at the site of injection (left-ventricles), a few cells could migrate from the ventricles to the glioma region. It was also noticed that the implanted labeled cells that remained in the ventricles were seen as a hypointense signal but with low signal intensity as compared to the day of implantation. This reduction in the signal intensity was reflected as a slight increase in the average T2 value - 47.8 msec- compared to that observed for the implanted labeled cells on Day 1 of implantation (39.2 msec). This could be due to the lower cell number (dilution) resulting from their diffusion to the CSF in ventricles or migration towards the tumor site.

Subsequently, after the first week and second weeks of transplantation, the size of the tumor mass was found to be increasing, with a higher number of dark spots appearing in the tumor region (yellow-dotted circles in Figure 3C and Figure 3D), indicating the gradual migration and infiltration of labeled MSCs into glioma. After two weeks, the average T2 value of the implanted labeled cells that remained in the ventricular region was further increased to 52.8 msec, which indicated the lowering of injected cell number due to their diffusion into ventricles or migration to the tumor. The average T2 value at the region of dark spots within the tumor area was 51.9 msec, which was lower than that of the other tumor region (58.8 msec). This difference in T2 value suggests that the migrated cells are distinguishable from the hyperintense tumor mass in MRI. However, compared to the injection site, the magnitude of the hypointense signal in the tumor is low, indicating that only a fraction of implanted cells migrated to the tumor. Unlike the injection site where the cells are aggregated, the tumor-migrated cells might be dispersed in the entire tumor mass, which could also result in this signal reduction.

The dilution of internalized nanoparticles within the proliferating cells can result in degradation and subsequent reduction in the MR signal. However, in the previous study, we evaluated the *in vitro* stability of nCP:Fe labeling during cellular proliferation by inspecting the retention of nanoparticles within the labeled stem cells at different time points (day 2, day 5, and day 7) using Prussian blue imaging, which clearly showed that the internalized nanoparticles were present within the proliferating stem cells, up to 7 days post-labeling. [26] In addition, the *in vivo* MR imaging of nCP:Fe labeled cells (1×10^6 cells) implanted intra-cerebrally in healthy rat brain showed detectable hypointense signal in T2/T2* weighted images for a prolonged period of up to 30 days [26]. These observations from the previous study suggest that nCP:Fe labeling enables detecting the stem cells as evident dark spots in T2/T2* weighted MR images up to 30 days *in vivo,* and hence, in the present study*,* the low MR signal observed in the tumor region after 14 days, might not be due to the dilution of nanoparticles within the labeled cells but could be due the small fraction of implanted stem cells migrated to the tumor region itself. Overall, the observations suggest that, although fewer in number, the intraventricularly administered stem cells could migrate to the glioma, which could be serially traced using MRI by nCP:Fe-labeling of cells.

To confirm the migration and presence of nCP:Fe labeled-MSC in the tumor region, we performed histological evaluation using alizarin-red (for Ca^{2+} in nCP:Fe) and Prussian-blue staining (for Fe^{3+} in nCP:Fe), two weeks post cell implantation (Figure 4). Consecutive brain tissue sections were used for staining. Figure 4A.1 and Figure 4A.2 represent the corresponding MRI images of the animal brain sections used for the histological staining. Dark signals near the injection site in T2*WI are labeled cells site-of-injection ('LC-SOI') and marked as '1' in both the MRI and histology images. The cells at similar positions in the corresponding brain section were positive for Prussian-blue staining, representing the labeled cells (LC) that remained in the injection path in the cerebral region. The high magnification image of these Prussian-positive cells (Figure 4B.1.a) observed in the injection path exhibited positional similarity with positively stained cells in the alizarin-red image (Figure 4B.1.b), indicating the presence of nCP:Fe labeled cells.

The Prussian-blue and alizarin-red stained images (Figure 4B.2.a and Figure 4B.2.b, respectively) confirmed that the hypointense signal in the lateral-ventricles seen in T2*WI (marked as '2' in Figure 4A.2) arises from the implanted-labeled cells (denoted as 'LC in ventricles'). It was also noticed that, at the tumor border (TB) near the ventricular region, a few cells were Prussian-blue positive (Figure 4B.2.a), which were well matched with alizarin-red positive cells in the adjacent section (Figure 4B.2.b), confirming the presence of migrated nCP:Fe labeled cells (M-LC) in the tumor margin. This showed the infiltration of LC from the ventricles to the tumor mass (TM), indicating the potential tumor-targeting property of stem cells. A few Prussian-blue-positive cells were seen within the TM (marked as '3' in Figure 4B), which was consistent with the prominent dark spots present within the tumor area in T2*WI (indicated by yellow-dotted circles and marked as '3' in Figure 4A.2). The high magnification image of these Prussian-blue positive cells within the tumor region (indicated by yellow-

dotted circles in Figure 4B.3.a) displayed positional similarity with alizarin-red positive cells (indicated by the yellow-dotted circle in Figure 4B.3.b) in the neighbouring section.

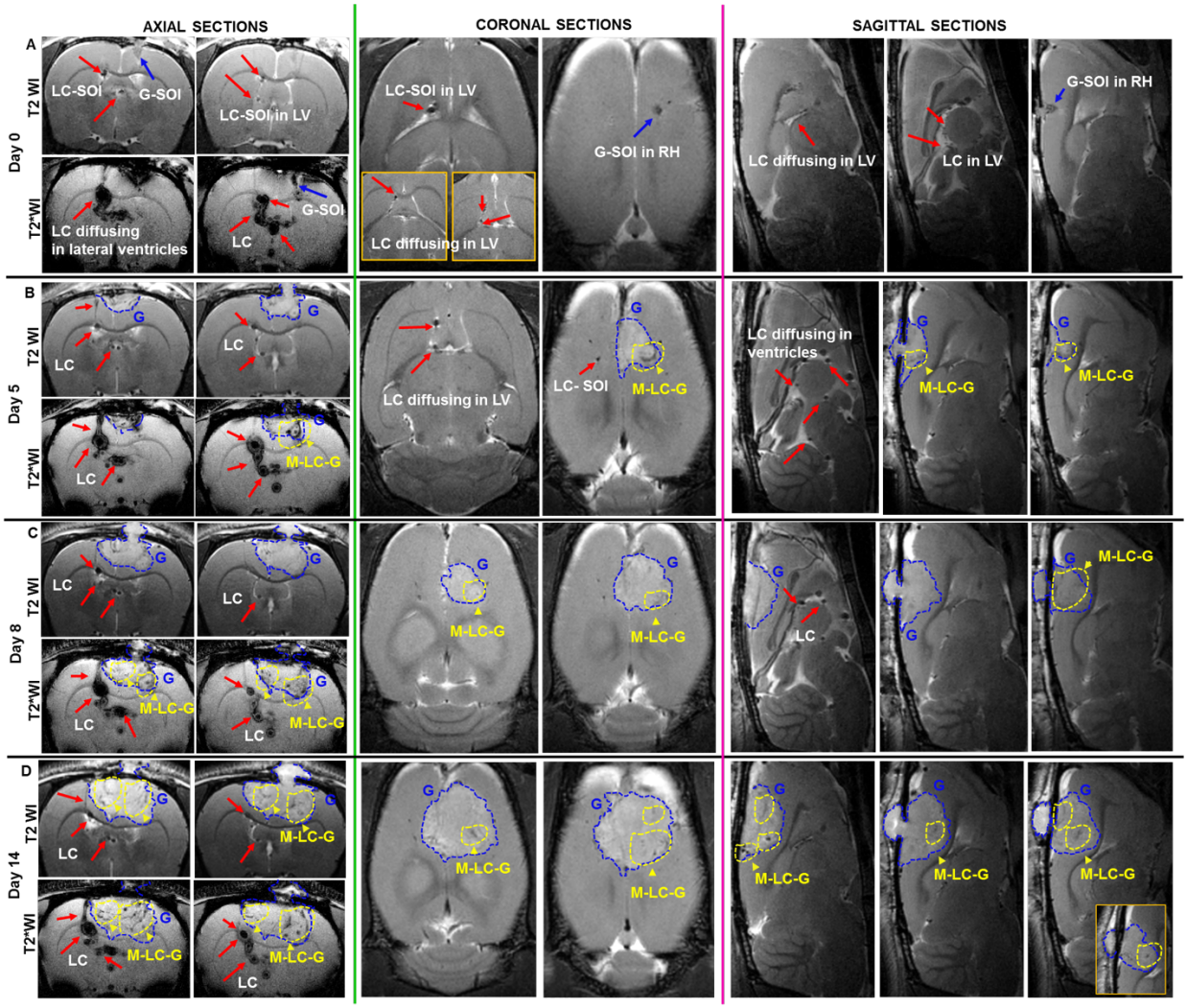

*Figure 3. In vivo MRI tracking of intra-ventricularly delivered nCP:Fe labeled MSCs towards glioma in a C6-glioma rat model. Axial T2WI and corresponding T2*WI of two consecutive brain sections along with their coronal and sagittal images A) immediately after delivery of labeled cells (Day 7- post inoculation of C6-glioma cells), B) 5 days, C) 8 days and D) 14 days post – labeled cell injection. nCP: Fe-labeled cells (LC) are indicated by red arrows, and the injection site of C6-glioma cells (G-SOI) is indicated by blue arrows. The intracranial glioma (G) is marked as blue dotted lines, and the migrated labeled cells to the glioma (M-LC-G) are indicated by yellow arrowhead and marked within yellow-dotted circles.*

Thus, the dual-staining suggested the presence of migrated and labeled stem cells in the glioma region (denoted as M-LC-G) and hence revealed the homing ability of stem cells towards tumors. Further, the histological evaluation also suggested that, as observed in MRI, only a small fraction of implanted stem cells could migrate to the tumor region. Several studies have demonstrated the ability of MSCs to migrate towards glioma in vitro and in vivo specifically.[33],[34] Though the exact mechanism underlying the tumor tropism of MSCs *in vivo* is not fully understood to date, various growth factors /chemokines and receptor interactions

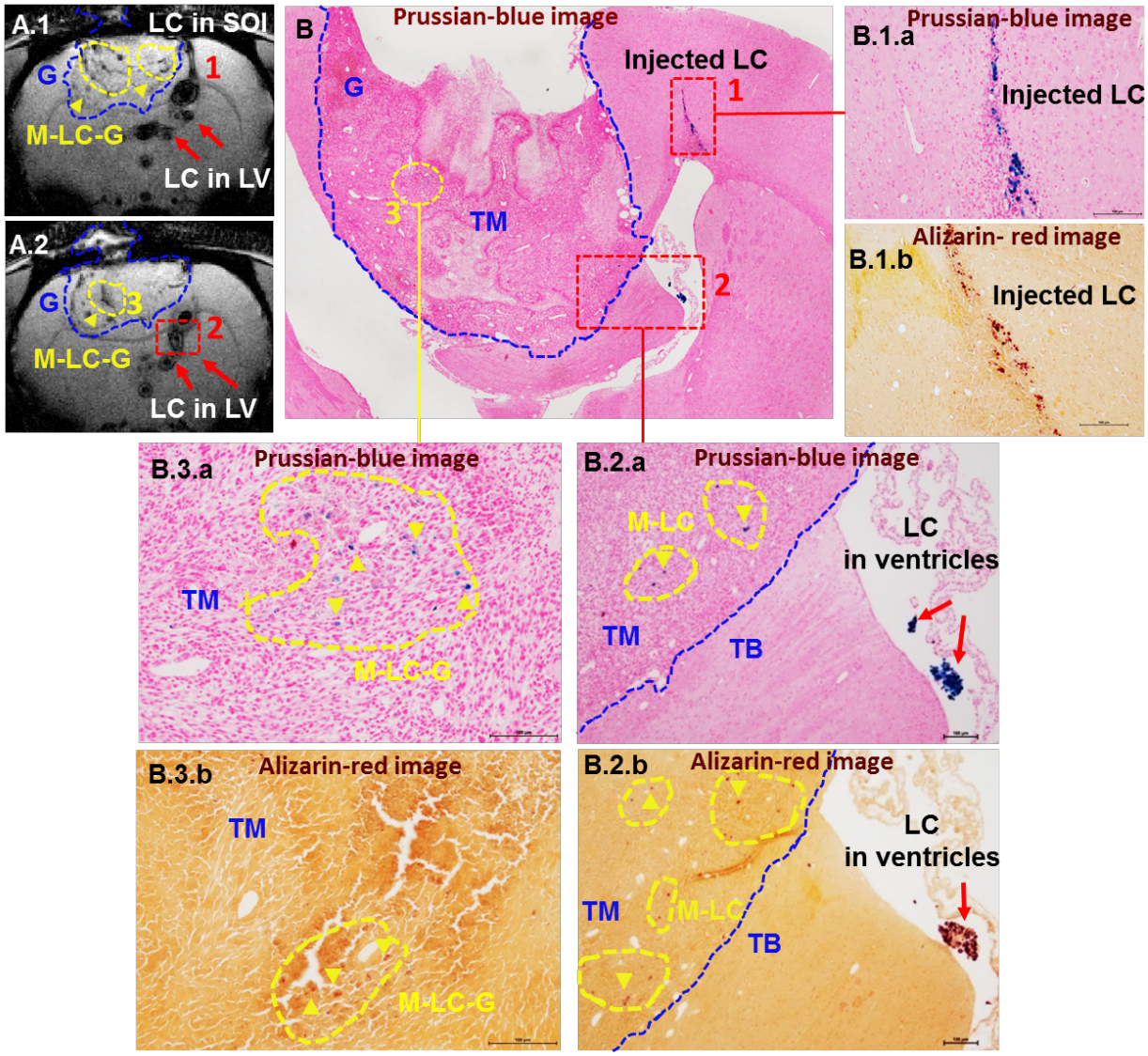

Figure 4. Histology of tumor migration of intra-ventricularly delivered nCP:Fe labeled MSCs towards glioma (after 14 days of cell implantation). A.1, A.2) T2 WI of two consecutive brain sections showing dark signal spots in the glioma region indicating the presence of labeled MSCs migrated to the tumor (the images are rotated 180° horizontally for comparing with histological images) B) Prussian-Blue staining of the corresponding brain section. The high magnification image of Prussian-positive cells (B.1.a) in the injection path (marked as '1' in Figure A.1 and Figure B) exhibiting positional similarity with positively stained cells in the alizarin-red stained image (B.1.b). The Prussian-blue (B.2.a) and alizarin-red stained images (B.2.b) show positively stained cells in the ventricular region. At the tumor border (TB) near the ventricular region, a few cells positive for Prussian blue staining (marked by yellow-dotted circles in B.2.a) were well matched with Alizarin red positive cells (B.2.b), indicating the migrated labeled cells (denoted as 'M-LC') from the ventricles into the tumor mass (TM). The high magnification image of Prussian-blue positive cells within the tumor mass (indicated by yellow-dotted circles in B.3.a) displays anatomical similarity with alizarin-red positive cells (indicated by yellow-dotted circles in B.3.b), indicating the presence of migrated nCP:Fe labeled MSCs, diffused within the tumor (denoted as 'M-LC-G').*

are proposed to be responsible for the tumor-tropic property of stem cells *in vitro*. [16],[33], [35] Our study demonstrated the possibility of imaging this tumor-targeting property of brain-implanted stem cells using nCP:Fe labelling-assisted-MRI.

In another aspect, the increase in tumor size with time (as seen from MR images) indicated

that the migrated stem cells exerted no apparent impact on tumor progression *in vivo*. Though a number of reports have studied the inhibitory effects of MSCs on tumor growth, the exact role of MSCs in suppressing or supporting tumor progression remains controversial.[36],[37] It will depend on different factors, such as the dosing of stem cells, its delivery route, and the tumor microenvironment.[38],[39] In our study, the relatively low number of stem cells reached at the tumor site might have been insufficient to inhibit the tumor growth. Moreover, the C6-glioma cells are aggressively growing tumor cells that could outperform the challenge of migrated MSCs. Therefore, the cell dose, cell-delivery routes, and methods of enhancing the migratory properties must be well examined and optimized to achieve an efficacious anti-tumor effect of MSCs. Also, detailed investigation to evaluate the tumor-targeting capacity of MSCs, their mechanism, and their effect on tumor progression are highly warranted.

Conclusions

In summary, our study demonstrated that the migration of MSCs towards intracranial glioma could be non-invasively tracked under MRI by labeling them using nCP:Fe nano-contrast agent. The *in vivo* study following the intra-ventricular administration of nCP:Fe labeled MSCs in an experimental orthotopic rat C6-glioma model showed that the infiltration and distribution of labeled stem cells into the glioma could be visualized as dark spots in T2/T2* weighted-MR images. However, a relatively small fraction of implanted cells arrived at the tumor site. To the best of our knowledge, this is the first report suggesting the possibility of using nCP:Fe labelling-based MRI to track and delineate the migratory pattern of stem cells towards glioma. We believe that nCP:Fe labeling of stem cells can be used to reliably track their tumor-homing capacity in real-time using MRI, which will help in optimizing MSC-mediated therapies for malignant glioma treatment.

Supporting Information

The Supporting Information includes the experimental section and the movie showing the *in vitro* co-culture of labeled MSCs with C6 glioma cells.

Author Contributions

IMA: conducted preparation of nano-contrast agent, *in vitro* and *in vivo* studies, and drafted the manuscript. GSG: conducted MRI imaging. AA: participated in the design of contrast agent synthesis. MM: conducted Prussian-blue and alizarin-red histology staining. SN: provided strategic guidance for the study, reviewed the manuscript, and suggested improvements. KB: evaluated and supervised the study. MK: designed and supervised the experiments and edited the manuscript. All authors have approved the final version of the manuscript.

Funding Sources

Ms. Ida M. Anna thanks ICMR-India for the funding through the Senior Research Fellowship (45/29/2018-NAN/BMS). This work was also supported by the Department of Biotechnology (DBT), Government of India, under the project “Translational Development of Protein Nanomedicine and Multifunctional Hydroxyapatite Nano-Contrast Agent” (BT/PR7665/NNT/28/658/2013).

Acknowledgment

The authors gratefully acknowledge Dr. A. Thennavan and Dr. Thajunnisa A. S for performing the animal surgical procedures for the *in vivo* studies. We also thank Mr. Sunilkumar O. R., Ms. Sunitha S, and Mr. Arun K. S for their technical assistance in conducting the animal surgeries. The authors thank Mr. Sajin P. Ravi and Mr. Dennis Mathew for their technical assistance in using a scanning electron microscope and confocal microscope, respectively.

Quote this article as Anna IM, Gowd GS, Ashokan A, Manohar M, Nair SV, Bhakoo K, and Koyakutty M, Magnetic resonance imaging of mesenchymal stem cell – migration towards glioblastoma using nano-calcium phosphate contrast agent, Precis. Nanomed. 2024, 7(1):1252-1263, https://doi.org/10.332/001c.94159.

References

[1] D. Bexell, A. Svensson, and J. Bengzon, "Stem cell-based therapy for malignant glioma," *Cancer Treat. Rev.*, vol. 39, no. 4, pp. 358–365, 2013, doi: 10.1016/j.ctrv.2012.06.006.

[2] M. S. S. Bovenberg, M. H. Degeling, and B. A. Tannous, "Advances in stem cell therapy against gliomas," *Trends Mol. Med.*, no. Box 1, pp. 1–11, 2012, doi: 10.1016/j.molmed.2013.03.001.

[3] Q. Zhang, W. Xiang, D. Yi, B. Xue, W. Wen, and A. Abdelmaksoud, "Current status and potential challenges of mesenchymal stem cell-based therapy for malignant gliomas," pp. 1–9, 2018.

[4] S.M. Kim, J.Y. Lim JY, S.I. Park, C.H. Jeong, J.H. Oh, M. Jeong, W. Oh, S.H. Park, Y.C. Sung and, S.S. Jeun, "Gene therapy using TRAIL-secreting human umbilical cord blood-derived mesenchymal stem cells against intracranial glioma," *Cancer Res.*, vol. 68, no. 23, pp. 9614–9623, 2008, doi: 10.1158/0008-5472.CAN-08-0451.

[5] M. Cao, J. Mao, X. Duan, L. Lu, F. Zhang, B. Lin, M. Chen, C. Zheng, X. Zhang and, J. Shen, "In vivo tracking of the tropism of mesenchymal stem cells to malignant gliomas using reporter gene-based MR imaging," *Int. J. Cancer*, vol. 142, no. 5, pp. 1033–1046, Mar. 2018, doi: 10.1002/ijc.31113.

[6] X. Wu, J. Hu, L. Zhou, Y. Mao, B. Yang, L. Gao, R. Xie, F. Xu, D. Zhang, J. Liu and, J. Zhu, "In vivo tracking of superparamagnetic iron oxide nanoparticle-labeled mesenchymal stem cell tropism to malignant gliomas using magnetic resonance imaging: Laboratory investigation," *J. Neurosurg.*, vol. 108, no. 2, pp. 320–329, 2008, doi: 10.3171/JNS/2008/108/2/0320.

[7] IA Ho, H.C. Toh, W.H. Ng, Y.L. Teo, C.M. Guo, K.M. Hui and, P.Y. Lam, "Human bone marrow-derived mesenchymal stem cells suppress human glioma growth through inhibition of angiogenesis," *Stem Cells*, vol. 31, no. 1, pp. 146–155, 2013, doi: 10.1002/stem.1247.

[8] C. Zhang, S.J. Yang, Q. Wen, J.F. Zhong, X.L. Chen, A. Stucky, M.F. Press and, X. Zhang, "Human-derived normal mesenchymal stem/stromal cells in anticancer therapies," *J. Cancer*, vol. 8, no. 1, pp. 85–96, 2017, doi: 10.7150/jca.16792.

[9] R. Ramasamy, E. W. F. Lam, I. Soeiro, V. Tisato, D. Bonnet, and F. Dazzi, "Mesenchymal stem cells inhibit proliferation and apoptosis of tumor cells: Impact on in vivo tumor growth," *Leukemia*, vol. 21, no. 2, pp. 304–310, 2007, doi: 10.1038/sj.leu.2404489.

[10] P. Barcellos-de-souza, V. Gori, F. Bambi, and P. Chiarugi, "Tumor microenvironment: Bone marrow-mesenchymal stem cells as key players," *BBA - Rev. Cancer*, 2013, doi: 10.1016/j.bbcan.2013.10.004.

[11] C. Review, D. Mesenchymal, S. Cells, and S. T. Growth, "T ISSUE -S PECIFIC S TEM C ELLS Concise Review : Dissecting a Discrepancy in the Literature : Do Mesenchymal Stem Cells Support or Suppress Tumor Growth ?," pp. 11–19, 2011, doi: 10.1002/stem.559.

[12] M. Hoehn, D. Wiedermann, C. Justicia, P. Ramos-Cabrer, K. Kruttwig, T. Farr and, U. Himmelreich, "Cell tracking using magnetic resonance imaging," *J. Physiol.*, vol. 584, no. 1, pp. 25–30, Oct. 2007, doi: 10.1113/jphysiol.2007.139451.

[13] J. W. M. Bulte and D. L. Kraitchman, "Iron oxide MR contrast agents for molecular and cellular imaging," *NMR Biomed.*, vol. 17, no. 7, pp. 484–499, Nov. 2004, doi: 10.1002/nbm.924.

[14] J. W. M. Bulte, "In vivo MRI cell tracking: clinical studies.," *AJR. Am. J. Roentgenol.*, vol. 193, no. 2, pp. 314–25, Aug. 2009, doi: 10.2214/AJR.09.3107.

[15] J. S. Jackson, J. P. Golding, C. Chapon, W. A. Jones, and K. K. Bhakoo, "Homing of stem cells to sites of inflammatory brain injury after intracerebral and intravenous administration: a longitudinal imaging study.," *Stem Cell Res. Ther.*, vol. 1, no. 2, p. 17, Jun. 2010, doi: 10.1186/scrt17.

[16] L.Y. Chien, J.K. Hsiao, S.C. Hsu, M. Yao, C.W. Lu, H.M. Liu, Y.C. Chen, C.S. Yang and, D.M. Huang, "In vivo magnetic resonance imaging of cell tropsim, trafficking mechanism, and therapeutic impact of human mesenchymal stem cells in a murine glioma model," *Biomaterials*, vol. 32, no. 12, pp. 3275–3284, 2011, doi: 10.1016/j.biomaterials.2011.01.042.

[17] F.T. Hsu, Z.H. Wei, Y.C. Hsuan, W. Lin, Y.C. Su, C.H. Liao, and C.L. Hsieh, "MRI tracking of polyethylene glycol-coated superparamagnetic iron oxide-labeled placenta-derived mesenchymal stem cells toward glioblastoma stem-like cells in a mouse model," *Artif. Cells, Nanomedicine Biotechnol.*, vol. 46, no. sup3, pp. S448–S459, 2018, doi: 10.1080/21691401.2018.1499661.

[18] S. J. H. Soenen, N. Nuytten, S. F. De Meyer, S. C. De Smedt, and M. De Cuyper, "High Intracellular Iron Oxide Nanoparticle Concentrations Affect Cellular Cytoskeleton and Focal Adhesion Kinase-Mediated Signaling," *Small*, vol. 6, no. 7, pp. 832–842, Apr. 2010, doi: 10.1002/smll.200902084.

[19] S. J. H. Soenen, U. Himmelreich, N. Nuytten, and M. De Cuyper, "Cytotoxic effects of iron oxide nanoparticles and implications for safety in cell labelling," *Biomaterials*, vol. 32, no. 1, pp. 195–205, Jan. 2011, doi: 10.1016/J.BIOMATERIALS.2010.08.075.

[20] Y.-X. J. Wang, "Current status of superparamagnetic iron oxide contrast agents for liver magnetic resonance imaging," *World J. Gastroentrology*, vol. 21, no. 47, pp. 13400–13402, 2015, doi: 10.3748/wjg.v21.i47.13400.

[21] Y. X. J. Wáng and J. M. Idée, "A comprehensive literatures update of clinical researches of superparamagnetic resonance iron oxide nanoparticles for magnetic resonance imaging," *Quant. Imaging Med. Surg.*, vol. 7, no. 1, pp. 88–122, 2017, doi: 10.21037/qims.2017.02.09.

[22] A. Ashokan, G.S. Gowd, V.H. Somasundaram, A. Bhupathi, R. Peethambaran, A.K. Unni, S. Palaniswamy, S.V. Nair, and M. Koyakutty M, "Multifunctional calcium phosphate nano-contrast agent for combined nuclear, magnetic and near-infrared in vivo imaging," *Biomaterials*, vol. 34, no. 29, pp. 7143–7157, Sep. 2013, doi: 10.1016/J.BIOMATERIALS.2013.05.077.

[23] A. Ashokan , V.H. Somasundaram, G.S. Gowd, I.M. Anna, G.L. Malarvizhi, B. Sridharan, R.B. Jobanputra, R. Peethambaran, A.K. Unni, S. Nair, and M. Koyakutty, "Biomineral Nano-Theranostic agent for Magnetic Resonance Image Guided, Augmented Radiofrequency Ablation of Liver Tumor," *Sci. Rep.*, vol. 7, no. 1, p. 14481, Dec. 2017, doi: 10.1038/s41598-017-14976-8.

[24] M. K. B. Sridharan, N. Devarajan, R. Jobanputra, G. S. Gowd, I. M. Anna, A. Ashokan, S. Nair, and M. Koyakutty "nCP:Fe Nanocontrast Agent for Magnetic Resonance Imaging-Based Early Detection of Liver Cirrhosis and Hepatocellular Carcinoma," *ACS Appl. Bio Mater.*, vol. 4, no. 4, pp. 3398–3409, 2021.

[25] A. A. M. Anoop, A. R. Nambiar, S. V. Nair, and M. Koyakutty, "Zoledronic acid conjugated calcium phosphate nanoparticles for applications in cancer immunotherapy," *Mater. Today Commun.*, vol. 30, no. 103065, 2022.

[26] I.M. Anna, B.N. Sathy, A. Ashokan, G.S. Gowd, R. Ramachandran, A.K. Kochugovindan Unni, M. Manohar, D. Chulliyath, S. Nair, K. Bhakoo, and M. Koyakutty, "nCP:Fe □ A Biomineral Magnetic Nanocontrast Agent for Tracking Implanted Stem Cells in Brain Using MRI," 2019, doi: 10.1021/acsabm.9b00709.

[27] J. A. Collins, C. A. Schandl, K. K. Young, J. Vesely, and M. C. Willingham, "Major DNA fragmentation is a late event in apoptosis," *J. Histochem. Cytochem.*, vol. 45, no. 7, pp. 923–934, 1997, doi: 10.1177/002215549704500702.

[28] M. C. Willingham, "Cytochemical methods for the detection of apoptosis," *J. Histochem. Cytochem.*, vol. 47, no. 9, pp. 1101–1109, 1999, doi: 10.1177/002215549904700901.

[29] J. Balvan, A. Krizova, J. Gumulec, M. Raudenska, Z. Sladek, M. Sedlackova, P. Babula, M. Sztalmachova, R. Kizek, R. Chmelik, and M. Masarik, "Multimodal holographic microscopy: Distinction between apoptosis and oncosis," *PLoS One*, vol. 10, no. 3, 2015, doi: 10.1371/journal.pone.0121674.

[30] Y.R. Lu,Y. Yuan, X.J. Wang, L.L. Wei, Y.N. Chen, C. Cong, S.F. Li, D. Long, W.D. Tan, Y.Q. Mao YQ, and J. Zhang, "The growth inhibitory effect of mesenchymal stem cells on tumor cells in vitro and in vivo," *Cancer Biol. Ther.*, vol. 7, no. 2, pp. 245–251, 2008, doi: 10.4161/cbt.7.2.5296.

[31] C. Yang, D. Lei, W. Ouyang, J. Ren, H. Li, J. Hu, and S. Huang, "Conditioned media from human adipose tissue-derived mesenchymal stem cells and umbilical cord-derived mesenchymal stem cells efficiently induced the apoptosis and differentiation in human glioma cell lines in vitro," *Biomed Res. Int.*, vol. 2014, 2014, doi: 10.1155/2014/109389.

[32] R. Ramachandran, V.R. Junnuthula, G.S. Gowd, A. Ashokan, J. Thomas, R. Peethambaran, A. Thomas, A.K. Unni, D. Panikar, S.V. Nair, and M. Koyakutty M, "Theranostic 3-Dimensional nano

brain-implant for prolonged and localized treatment of recurrent glioma," *Sci. Rep.*, vol. 7, p. 43271, Mar. 2017, doi: 10.1038/srep43271.

[33] Q.-H. A. Kosztowski T, Zaidi HA, "Applications of neural and mesenchymal stem cells in the treatment of gliomas," *Expert Rev*, vol. 9, no. 5, pp. 597–612, 2009.

[34] K. Nakamura, Y. Ito, Y. Kawano, K. Kurozumi, M. Kobune, H. Tsuda, A. Bizen, O. Honmou, Y. Niitsu, and H. Hamada, "Anti-tumor effect of genetically engineered mesenchymal stem cells in a rat glioma model," *Gene Ther.*, vol. 11, no. 14, pp. 1155–1164, 2004, doi: 10.1038/sj.gt.3302276.

[35] S.M. Kim, D.S. Kim, C.H. Jeong, D.H. Kim,J.H. Kim, H.B. Jeon, S.J. Kwon, S.S. Jeun, Y.S. Yang, W. Oh, and J.W. Chang, "CXC chemokine receptor 1 enhances the ability of human umbilical cord blood-derived mesenchymal stem cells to migrate toward gliomas," *Biochem. Biophys. Res. Commun.*, vol. 407, no. 4, pp. 741–746, 2011, doi: 10.1016/j.bbrc.2011.03.093.

[36] H. Y. Lee and I. S. Hong, "Double-edged sword of mesenchymal stem cells: Cancer-promoting versus therapeutic potential," *Cancer Sci.*, vol. 108, no. 10, pp. 1939–1946, 2017, doi: 10.1111/cas.13334.

[37] K. J. Rhee, J. I. Lee, and Y. W. Eom, "Mesenchymal stem cell-mediated effects of tumor support or suppression," *Int. J. Mol. Sci.*, vol. 16, no. 12, pp. 30015–30033, 2015, doi: 10.3390/ijms161226215.

[38] A. Bajetto, S. Thellung, F. Barbieri, T. Florio, and I. Dellacasagrande, "Cross talk between mesenchymal and glioblastoma stem cells : Communication beyond controversies," doi: 10.1002/sctm.20-0161.

[39] Z. Sun, S. Wang, and R. C. Zhao, "The roles of mesenchymal stem cells in tumor inflammatory microenvironment," *J. Hematol. Oncol.*, vol. 7, no. 1, pp. 1–10, 2014, doi: 10.1186/1756-8722-7-14.